Available online at www.sciencedirect.com
SCIENCE DIRECT
Journal of Physics and Chemistry of Solids 67 (2006) 1379–1386
JOURNAL OF PHYSICS AND CHEMISTRY OF SOLIDS
www.elsevier.com/locate/jpcs

AC-conductivity and Raman spectra of polyiodide inclusion compounds (β-cyclodextrin)$_2 \cdot KI_7 \cdot 16H_2O$ and (β-cyclodextrin)$_2 \cdot LiI_7 \cdot 14H_2O$ during the dehydration process

John C. Papaioannou*, Vasileios G. Charalampopoulos, Pantelis Xynogalas, Kyriakos Viras

Department of Chemistry, Laboratory of Physical Chemistry, National and Kapodistrian University of Athens, PO Box 64004, 157 10 Zografou, Athens, Greece

Received 15 June 2005; received in revised form 24 January 2006; accepted 25 January 2006

Abstract

The frequency and temperature dependence of ac-conductivity and phase shift of polycrystalline inclusion compounds (β-CD)$_2 \cdot KI_7 \cdot 16H_2O$ and (β-CD)$_2 \cdot LiI_7 \cdot 14H_2O$ (β-CD = β-cyclodextrin) has been investigated over the frequency and temperature ranges of 0–100 kHz and 240–420 K. A Raman spectroscopic study and calorimetric measurements are also accomplished. The Arrhenius exponential behaviour $\sigma = \sigma_0 \exp\left(-E_W/2K_BT\right)$ of the ac-conductivity for $T > 275$ K is caused by the contribution of the metal cations K^+, Li^+. This contribution is facilitated by the water-net via the Grotthuss mechanism. The ac conductivity starts deviating from the exponential behaviour with lower increasing rate, at 347 K for β-K and at 353 K for β-Li reaching a maximum value at 371.1 and 361.8 K, respectively, and then decreases rapidly due to the gradual removal of all the water molecules. The values 371.1 and 361.8 K are characterized as semiconductor to metal transition temperatures. The shift of the initial Raman peak at 179 cm^{-1} to the final value 165 cm^{-1} as the temperature increases reveals the lengthening of I_2 units via a charge transfer interaction in I_7^- units. A second topical maximum value of conductivity appears at 399.7 K for β-K and 403 K for β-Li, attributed to the sublimation of I_2.

1. Introduction

It has been shown [1,2] that when α-, β-cyclodextrins (α-CD, β-CD) are crystallized from aqueous solutions with metal iodide/iodine, channel-type inclusion compounds are formed in which α-CD or β-CD molecules, are stacked in a head-to-head arrangement to produce dimers in whose tubular cavities polyiodide chains are developed. α-CDs give four different types of crystals (triclinic, tetragonal, pseudo-hexagonal, hexagonal) depending on the nature of the metal in contrast to β-CDs, which display only one crystal lattice type (monoclinic $P2_1$) for a variety of metals. The crystal structure of β-CD with K^+, shows that the polyiodide chain consists of I_7^- units which can be formulated as $I_2 \cdot I_3^- \cdot I_2 \ldots$ shaped into a Z-like structure in which both I_2 units are nearly perpendicular to the I_3^- unit [3].

We have investigated the dielectric relaxation properties of the α-CD inclusion compounds with lithium, cadmium, barium and potassium metals in the temperature region 120–300 K [4,5]. We have also investigated the dielectric relaxation properties of the β-CD inclusion compounds with potassium and lithium metals named β-K, β-Li, respectively, in the temperature region 120–300 K [6]. Concerning β-K, β-Li, the temperature dependence of the dielectric constant (real part ε' and imaginary part ε'') and phase shift φ showing two steps, two peaks and two minima, respectively, reveals the existence of two kinds of water molecules (tightly bound and easily movable). The two systems exhibit the order–disorder transition that according to Betzel, et al., [7,8] is caused by the transformation of flip-flop hydrogen bonds to the normal state. Both samples for $T > 275$ K show semiconductive behaviour with energy gaps 0.72 eV for β-Li and 0.58 eV for β-K calculated from the Arrhenius equation $\sigma = \sigma_0 \exp\left(-E_W/2K_BT\right)$.

*Corresponding author.
E-mail address: jpapaioannou@chem.uoa.gr (J.C. Papaioannou).

0022-3697/$ - see front matter © 2006 Elsevier Ltd. All rights reserved.
doi:10.1016/j.jpcs.2006.01.109

The above results of the previous article [6] correspond to the temperature region $T<300\,K$, where all the water molecules exist in the crystal lattice. At higher temperatures additional effects appear in the electrical properties of β-K and β-Li, related to the abrupt increase of the conductivity, the removal of the water molecules and the contribution of the polyiodide chain. Because of the high conductivity values, the dielectric parameters ε', ε'' are no longer sensitive to depict these effects. On the contrary, the temperature dependence of the phase shift φ and the ac-conductivity σ detects all the different processes taking place in the sample. So in the present work we investigate the variation of the ac-conductivity and the phase shift of the β-cyclodextrin–polyiodide inclusion compounds $(\beta\text{-CD})_2\cdot KI_7\cdot 16H_2O$ and $(\beta\text{-CD})_2\cdot LiI_7\cdot 14H_2O$, over the frequency range 0–100 kHz and the temperature region 240–420 K. Moreira da Silva et al. [9] have investigated the hydration and dehydration processes of β-cyclodextrin. They found a linear relationship between the intensity of the Raman band νOH ($\sim$3350 cm^{-1}) and the ambient humidity. In our case the dehydration process is determined by calorimetric measurements in the temperature region 300–420 K, whereas the Raman spectroscopic study is focused on the range 140–210 cm^{-1} in which the polyiodide interactions take place.

2. Experimental

β-Cyclodextrin, iodine, lithium iodide and potassium iodide were purchased from Fluka Chemica. The preparation of both samples was carried out according to Ref. [2]. One gram of β-CD was dissolved in 80 ml of distilled water at room temperature under stirring until the solution became almost saturated. Then 0.38 g potassium iodide and 0.44 g solid iodine were added simultaneously to the solution and it was heated to 70 °C for 20–25 min. The hot solution was filtered and left in a Dewar flask containing water at the same temperature. After 2 days, very fine reddish-brown thin needles of β-K were grown, held back in a Buchner filter and dried in air. For β-Li we used 1 g β-CD, 0.30 g lithium iodide and 0.44 g solid iodine, and reddish-brown thin needles β-Li were grown in a similar way as the β-K case. The water content of the crystals was determined by the use of thermogravimetric analysis (NETZSCH-STA 409 EP, Controller TASC 414/3, heating rate 5 °C min^{-1}). β-K and β-Li were found to contain 16 and 14 water molecules per dimer, respectively (Fig. 1). So the general compositions are $(\beta\text{-CD})_2\cdot KI_7\cdot 16H_2O$ and $(\beta\text{-CD})_2\cdot LiI_7\cdot 14H_2O$. The numbers of water molecules in the present work were found higher than those reported [6], because in the present case the drying process took place in air, while in the previous case where an oven of 50–60 °C was used, some easily movable water molecules escaped.

Pressed pellets of powdered samples, 20 mm in diameter with thickness 1.00 mm for β-K and 1.05 mm for β-Li, were prepared with a pressure pump (Riken Power model P-1B) at room temperature. Two platinum foil electrodes were pressed at the same time with the sample.

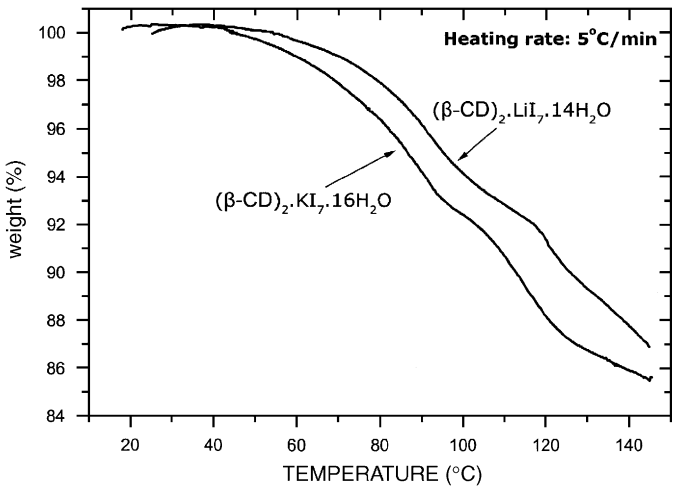

Fig. 1. Thermogravimetric analysis (TGA) of $(\beta\text{-CD})_2\cdot KI_7\cdot 16H_2O$ and $(\beta\text{-CD})_2\cdot LiI_7\cdot 14H_2O$.

The dielectric measurements were taken using a low-frequency (0–100 kHz) dynamical signal analyser (DSA-Hewlett-Packard 3561A), at the temperature range of 240–420 K, which was connected to a personal computer for further processing of the data stored in the DSA. An analytical description of the process is given in a previous article [10]. The differential scanning calorimetry (DSC) method (Perkin Elmer DSC-4 instrument) was used with a thermal analysis data station (TADS) system for all calorimetric measurements.

The Raman spectra were obtained at 4 cm^{-1} resolution from 3500 to 100 cm^{-1} with data point interval of 1 cm^{-1} using a Perkin-Elmer NIR FT-spectrometer (Spectrum GX II) equipped with an InGaAs detector. The measurements were performed in a temperature range of 30–150 °C (303–423 K). The laser power and spot (Nd:YAG at 1064 nm) were controlled to be constant at 50 mW during the experiments. Five hundred scans were accumulated and back scattering light was collected.

X-ray powder diffraction patterns were obtained with a Siemens D 5000 diffractometer (Cu Kα1 = 1.5406 Å, Cu Kα2 = 1.5444 Å, scan range: 5–55° 2θ, monochromator:-graphite crystal, scan speed: 0.045 2θ s^{-1}). The calculation of the theoretical X-ray powder diffraction pattern was performed by the computer program Powder Cell 2.3 developed by Nolze and Kraus [11], using the single crystal $(\beta\text{-CD})_2\cdot KI_7\cdot 9H_2O$ diffraction data reported by Betzel et al. in Ref. [3].

3. Results

3.1. Temperature dependence of conductivity and phase shift

The conductivity was calculated from the impedance measurements according to

$$\sigma = 4h\,(\pi D^2)^{-1} G = 4h\,(\pi D^2)^{-1}\ \mathrm{Re}\ Z\left(|Z|^{-2}\right), \qquad (1)$$

where h is the thickness, D the diameter, G the conductance and Z the complex impedance (Re Z the real part) of the sample [12].

The temperature variation of conductivity over the temperature range 240–420 K at frequency 300 Hz is shown in Fig. 2 for the inclusion compounds $(\beta\text{-CD})_2 \cdot KI_7 \cdot 16H_2O$ and $(\beta\text{-CD})_2 \cdot LiI_7 \cdot 14H_2O$.

In the case of β-K, the conductivity starts from an almost zero value at low temperatures 250–280 K, then increases by the temperature to a maximum value $4.83 \times 10^{-8}\,\Omega^{-1}\,cm^{-1}$ at 371.1 K, followed by a rapid decrease to the value $1.24 \times 10^{-8}\,\Omega^{-1}\,cm^{-1}$ at 391.3 K and finally increases to a second maximum value $1.35 \times 10^{-8}\,\Omega^{-1}\,cm^{-1}$ located at 399.7 K. The same behaviour is also observed for the β-Li. The conductivity increases by temperature to a maximum value $3.95 \times 10^{-7}\,\Omega^{-1}\,cm^{-1}$ located at 361.8 K, then it drops rapidly to $5.05 \times 10^{-8}\,\Omega^{-1}\,cm^{-1}$ at 391.3 K and increases again to a secondary maximum value $5.63 \times 10^{-8}\,\Omega^{-1}\,cm^{-1}$ at 403 K. For higher applied frequencies, the conductivity has higher values but the temperatures at which the peak values are observed remain unchanged.

The phase shift vs. temperature plot of β-K, β-Li samples is shown in Fig. 3. In the β-K case there are two minimum values 5.5° and 7.5° at the corresponding temperatures 371.1 and 399.7 K, respectively, at which the maximum peak values of σ vs. T plot were observed. Similar results are also observed for the β-Li sample with minimum values of phase shift 6.5° at 361.8 K and 8.6° at 403 K. For higher applied frequencies the phase shift φ has lower values but the temperatures at which the minima are observed remain unchanged.

3.2. Impedance plots (Cole–Cole)

The representative impedance plots of β-K, β-Li (Figs. 4 and 5) at temperatures 303.7 and 300.2 K, respectively, show a depressed semicircle in the frequency range

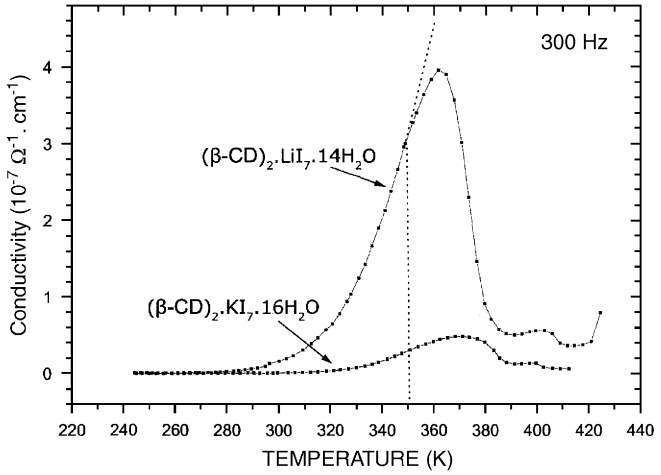

Fig. 2. Temperature dependence of the ac-conductivity of $(\beta\text{-CD})_2 \cdot KI_7 \cdot 16H_2O$ and $(\beta\text{-CD})_2 \cdot LiI_7 \cdot 14H_2O$ at 300 Hz.

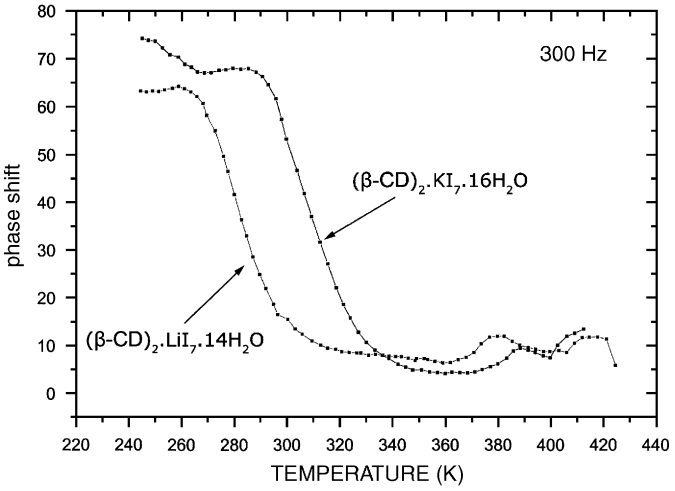

Fig. 3. Temperature dependence of the phase shift of $(\beta\text{-CD})_2 \cdot KI_7 \cdot 16H_2O$ and $(\beta\text{-CD})_2 \cdot LiI_7 \cdot 14H_2O$ at 300 Hz.

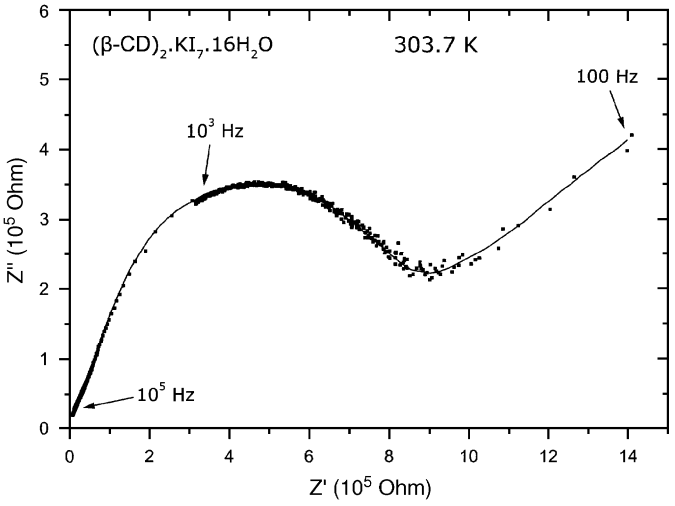

Fig. 4. Representative impedance plot of $(\beta\text{-CD})_2 \cdot KI_7 \cdot 16H_2O$ at 303.7 K.

300 Hz–100 kHz.At lower frequencies (less than 300 Hz) there is a linear response indicative of a diffusion process.

3.3. Calorimetric measurements

The DSC trace of β-K (Fig. 6) with scan rate $10^\circ\,min^{-1}$ shows one distinct endothermic peak with onset temperature 117 °C (390 K) over a temperature range of 50 °C and a shoulder at 127 °C (400 K). In a similar way the DSC trace of β-Li shows a main endothermic peak with onset temperature 108 °C (381 K) over a range of 40 °C and two shoulders at 119 °C (392 K) and 129 °C (402 K).

3.4. Raman Spectra

The Raman spectra of β-K inclusion compound in Fig. 7(a, b) for different temperatures 30, 50, 60, 70, 80, 90, 110, 120, 130, 140, 150 and 160 °C displays a strong band at

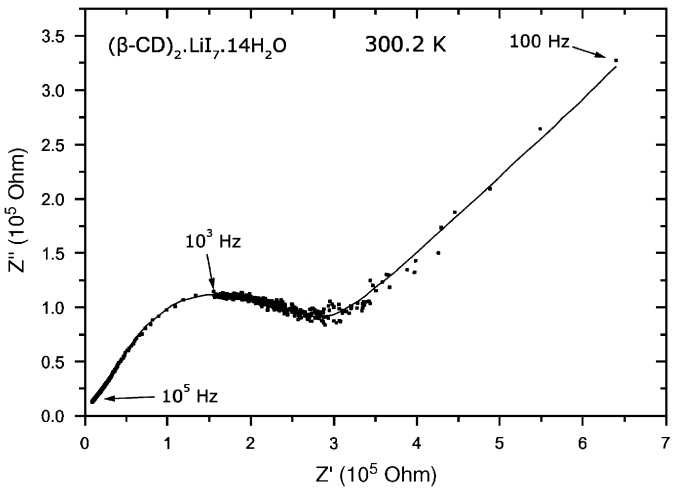

Fig. 5. Representative impedance plot of $(\beta\text{-CD})_2 \cdot LiI_7 \cdot 14H_2O$ at 300.2 K.

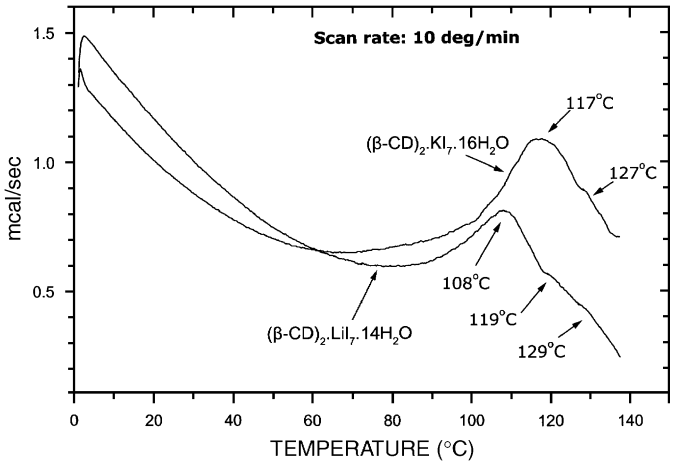

Fig. 6. DSC thermograms of $(\beta\text{-CD})_2 \cdot KI_7 \cdot 16H_2O$ and $(\beta\text{-CD})_2 \cdot LiI_7 \cdot 14H_2O$: heating rate $10^\circ\,min^{-1}$.

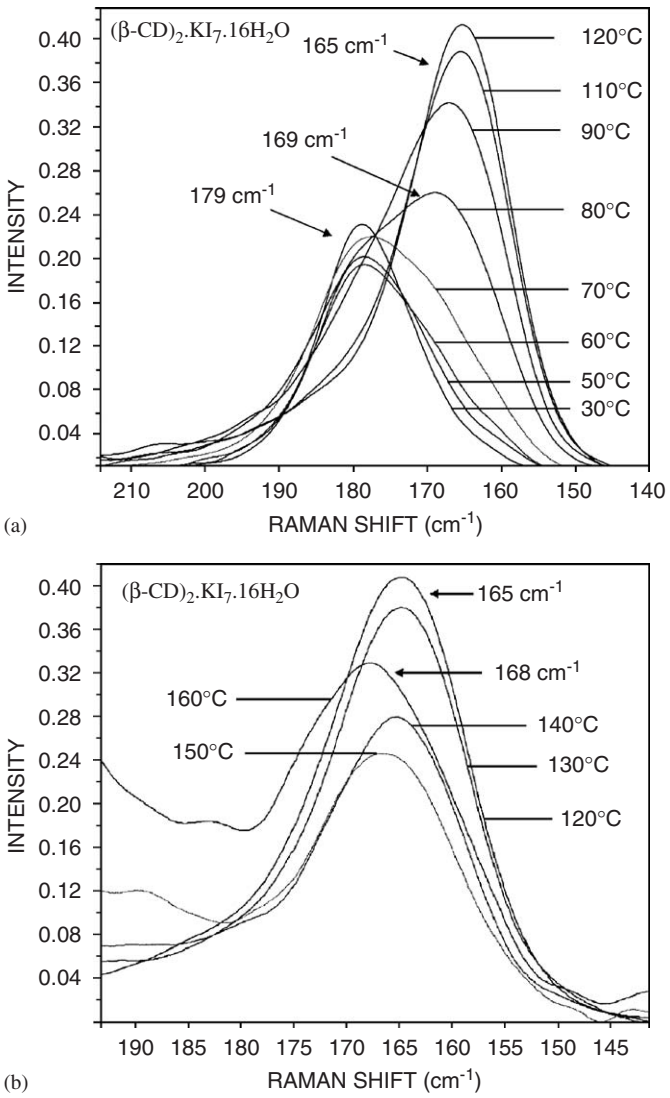

Fig. 7. Raman spectra of $(\beta\text{-CD})_2 \cdot KI_7 \cdot 16H_2O$ in the temperature range (a) 30–120 °C (b) 120–160 °C.

179 cm^{-1} at 30 °C with gradually decreasing intensity as the temperature increases. At 70 °C a shoulder arises at 169 cm^{-1} (0.17) with increasing intensity by temperature, which is shifted to the value 165 cm^{-1} in the temperature range 110–140 °C. The intensity takes a maximum value at 120 °C (0.41) and then decreases in the temperature range 130–150 °C (0.25). Finally, at 160 °C a band at 168 cm^{-1} is observed with increased intensity (0.33).

Fig. 8(a–d) shows the Raman spectra of β-Li for the different temperatures 30, 50, 70, 80, 90, 100, 110, 120, 130, 140 and 150 °C. It displays a strong band at 179 cm^{-1} for temperature 30 °C with decreasing intensity by temperature in the range 30–70 °C. For temperature 90 °C a broad double band is observed at 179 cm^{-1} (0.12) and 170 cm^{-1} (0.13) and a small shoulder arises at 163 cm^{-1}. For temperature 100 °C, three bands are observed at 179 cm^{-1} (0.09), 170 cm^{-1} (0.11) and 164 cm^{-1} (0.10). In the temperature range 110–120 °C, there is only one strong band at 165 cm^{-1} with gradually increasing intensity by temperature to the value 0.155, and then gradually decreasing intensity in the temperature range 130–140 °C to the value 0.14. Finally, at 150 °C a double broad band at 168 cm^{-1} and 163 cm^{-1} is observed.

3.5. X-ray powder diffraction

Fig. 9(a–c) shows the experimental X-ray powder diffraction patterns of $(\beta\text{-CD})_2 \cdot LiI_7 \cdot 14H_2O$, $(\beta\text{-CD})_2 \cdot KI_7 \cdot 16H_2O$ inclusion compounds and the simulated pattern calculated from the single-crystal X-ray diffraction data of $(\beta\text{-CD})_2 \cdot KI_7 \cdot 9H_2O$ [3]. It is obvious that β-Li and β-K exhibit similar XRD patterns (Bragg reflections at the same 2θ angles) which are in good agreement with the calculated of β-K. Therefore, the two complexes are isomorphous as it was foretold by Betzel et al., [3]. The appeared hump around 25° in (a) and (b) is caused by the presence of some amorphous material, while the multitude of peaks at higher 2θ angles is not a result of phase

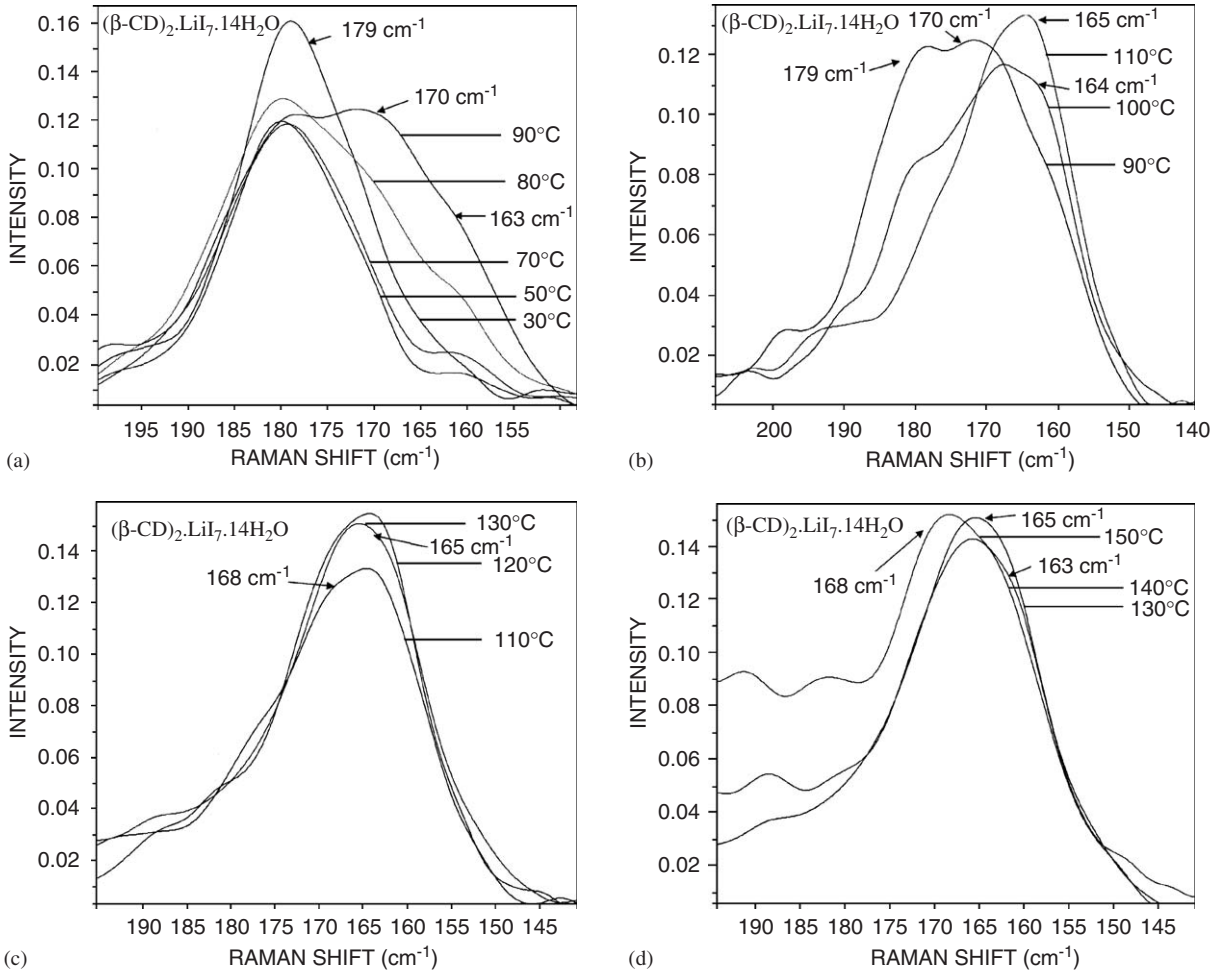

Fig. 8. Raman spectra of $(\beta\text{-CD})_2 \cdot LiI_7 \cdot 14H_2O$ in the temperature range (a) 30–90 °C (b) 90–110 °C (c) 110–130 °C (d) 130–150 °C.

impurities but corresponds to weak Bragg reflections as it is depicted in the calculated pattern (c). Some diffraction peaks exhibit larger relative intensities than those of the simulated pattern owing to the non-random distribution of crystal orientations (preferred orientation effects). We note that the presence of non-crystalline material (XRD hump) does not affect the macroscopic dielectric properties, since the fundamental building blocks (β-CD dimers, coordinated metal ions and I_7^- units) are expected to be unchanged.

4. Discussion

It has been shown [6] that the temperature dependence of conductivity of both inclusion compounds β-K and β-Li in the $\ln\sigma$ vs. $1/T$ plot shows a linear part at $T > 275$ K which is caused mainly by the activation and movement of metallic cations K^+ and Li^+ and is described by the Arrhenius

$$\sigma = \sigma_0 \exp\left(-E_W/2K_B T\right), \quad (2)$$

where E_W is the corresponding energy gap of the semiconductor. The metallic movements are clearly shown by the linear responses in the Cole–Cole plots (Figs. 4 and 5) [13].

The plot σ vs. T of Fig. 3 shows that the conductivity of β-K at 347 K (74 °C) starts deviating from the above exponential behaviour with smaller increasing rate, because of a second mechanism which decreases the conductivity by increasing temperature. At $T > 371.1$ K, the second mechanism becomes the predominant one, resulting in the transformation of the semiconductive character (σ increases by T) to metallic (σ decreases by T). So, 371.1 K can be characterized as a semiconductor to metal transition temperature.

We consider that the decreasing rate of conductivity is due to the removal of the water molecules. In the beginning of the heating process all the 16 water molecules per dimer occupy interstitial lattice positions. The K^+ cation is fourfold coordinated by two water molecules and by two O(6) hydroxyl groups in a near-tetrahedral arrangement, located between the β-CD dimers close to the I_3^- unit of the polyiodide chain [3]. As the temperature increases and the water molecules become easily movable, the above tetrahedral configuration is being perturbed and the metal cations K^+ are free to oscillate back and forth with the

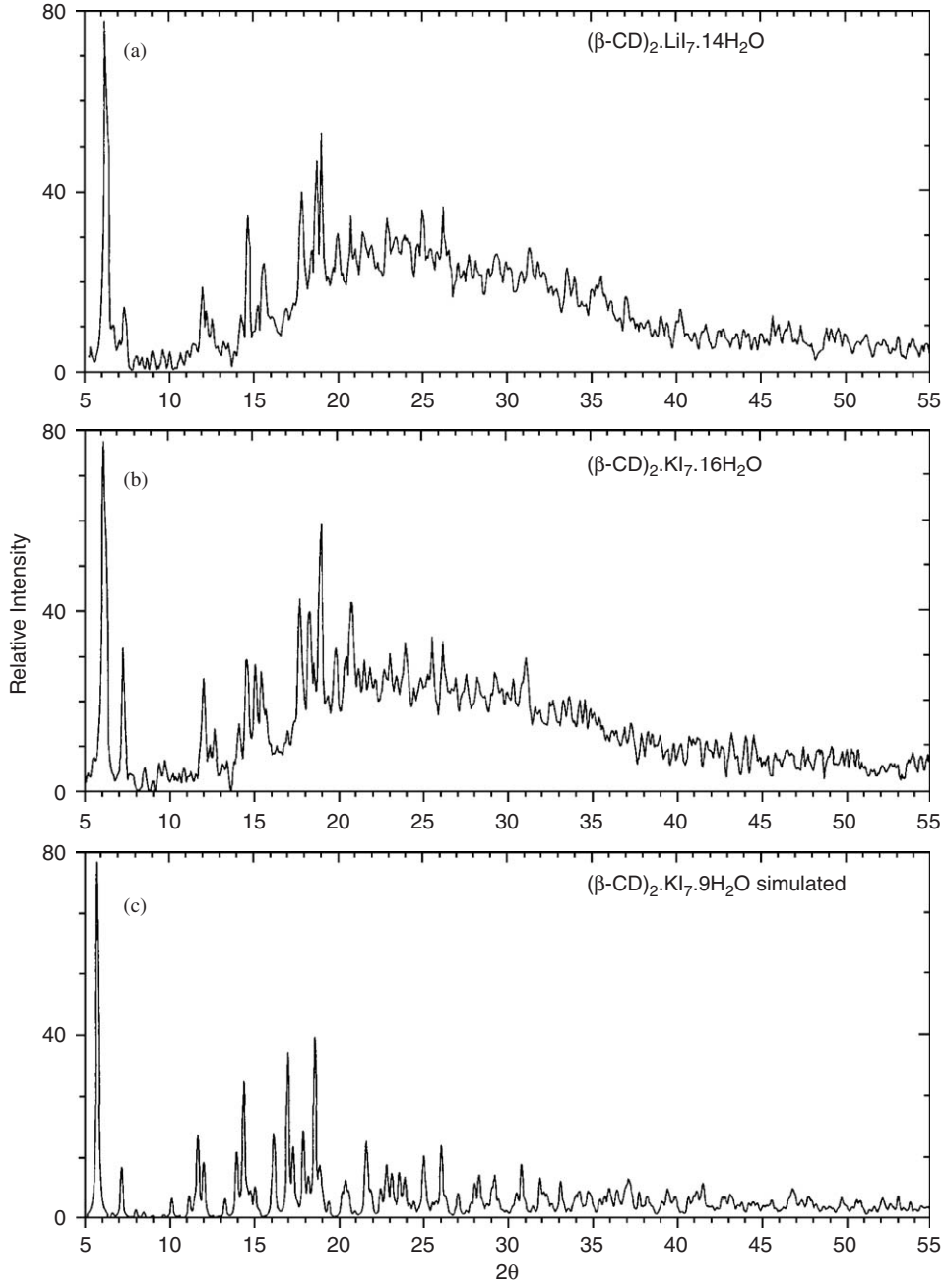

Fig. 9. (a),(b) Experimental X-ray powder diffraction patterns of $(\beta\text{-CD})_2 \cdot LiI_7 \cdot 14H_2O$ and $(\beta\text{-CD})_2 \cdot KI_7 \cdot 16H_2O$, respectively, and (c) calculated X-ray powder diffraction pattern from the single crystal data of $(\beta\text{-CD})_2 \cdot KI_7 \cdot 9H_2O$.

frequency of the applied alternate field, contributing to the rapid increase of conductivity. This contribution is facilitated by the net of the water molecules via the Grotthuss mechanism [14,15]. When the water molecules start to escape (70 °C) the ac-conductivity starts deviating from the exponential behaviour due to the rupture of the water-net, reaching a maximum value at $T = 371.1$ K and then decreasing rapidly because of the removal of all the remaining tightly bound water molecules. This explanation is also confirmed by the DSC trace of β-K (Fig. 6) showing a slab endothermic peak at 117 °C over the temperature region 70–125 °C, attributed to the removal of all 16 water molecules per dimer. This process renders the K^+ ions localized charges, having no contribution to the conductivity any more. At higher than 127 °C (400 K) temperatures sublimation of iodine takes place which is responsible for the topical maximum value of conductivity at 399.7 K (Fig. 2) and for the second shoulder of DSC trace at 127 °C (Fig. 6).

Additional information is found from the temperature dependence of the Raman spectra (Fig. 7). Initially in the range 30–70 °C, where all water molecules exist in the

lattice, the Raman spectra exhibit the band at 179 cm^{-1} with intensity decreasing by temperature. At higher than 70 °C temperatures a second band at 169 cm^{-1} coexists with the initial band at 179 cm^{-1} and finally at temperatures higher than 120 °C where all the water molecules have been removed, it is shifted to the value 165 cm^{-1} with intensity increasing by temperature. The above Raman bands are due to the polyiodide chain $I_2 \cdot I_3^- \cdot I_2$ and reflect the interactions between the I_3^- and the two I_2 units in each dimer [16,17]. Each I_2 unit is enclosed in each cavity of β-CD dimer, whereas the I_3^- unit is located between two β-CD dimers [3]. The iodine atoms I(1), I(2) of the central I_3^- unit show full occupance (1.0) with I(1)–I(2) separation 3.003 Å (Fig. 10). The atoms I(4), I(5) of I_2 units are disordered in positions with main occupancies I(4A) = 0.89 and I(5A) = 0.70 and positions with minor occupancies I(4B) = 0.15 and I(5B) = 0.14. In the case of main occupancies,the separation distance of iodine atoms in I_2 units is I(4A)–I(5A) = 2.77 Å and the separation between I_2 and I_3^- units is I(2)–I(4A) = 3.61 Å.In the case of minor occupancies,the corresponding positions display shorter distances (not estimated in the crystal structure).

A linear correlation of FT-Raman frequencies v(I–I) vs. the d(I–I) bond distances has been obtained for different weak complexes with I_2 [18]. As the interiodine distance

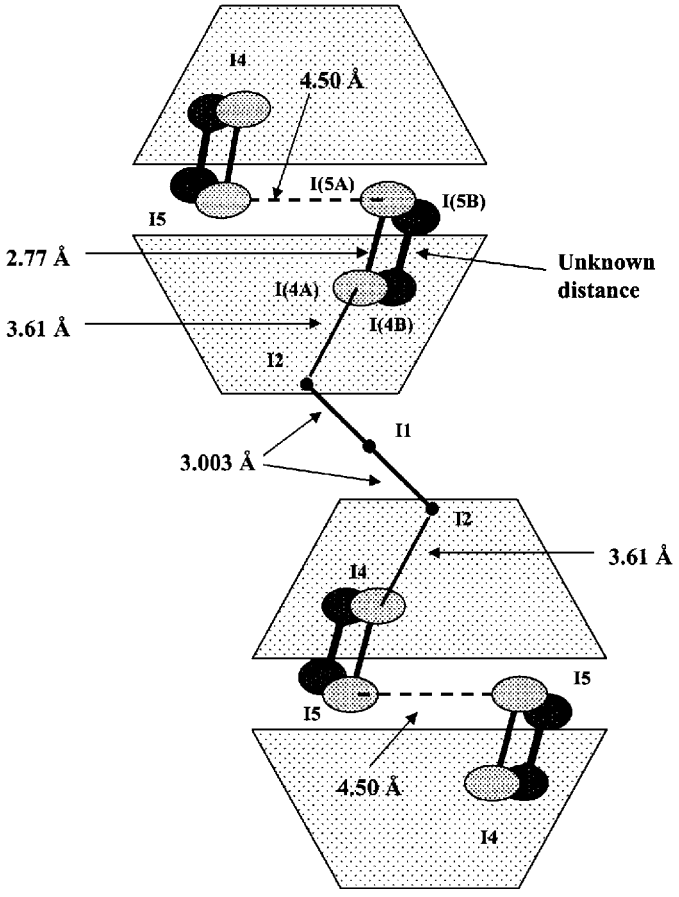

Fig. 10. Geometry of the polyiodide chain per cyclodextrin dimer in (β-CD)$_2 \cdot KI_7 \cdot 9H_2O$, according to Ref. [3].

increases, the FT-Raman band moves to lower frequency with respect to the value 180 cm^{-1} reported for solid iodine [19]. The Raman bands at 179 cm^{-1}, 169 cm^{-1} and 165 cm^{-1} found experimentally in Fig. 7 correspond to d(I–I) distances 2.72 Å, 2.75 Å and 2.77 Å, respectively. According to this, the strong band at 165 cm^{-1} could be assigned to the two disordered atoms of I_2 units I(4A), I(5A) with the longer distances I(4A)–I(5A) = 2.77 Å, while the initial band at 179 cm^{-1} to an average d(I–I) distance 2.72 Å, resultant of the simultaneous main and minor occupancies of iodine atoms I(4A), I(5A) and I(4B), I(5B) in the dimers. The same bands 178 and 166 cm^{-1} were observed in the case of another heptaiodide complex $[PPh_4]^+I_7$ that have been assigned to "the asymmetric stretches of the I···I–I units with a large component from the I–I interaction" [18]. The band at 169 cm^{-1} corresponding to d(I–I) = 2.75 Å is attributed to an intermediate state in which a charge transfer interaction $I_2 \cdots I_3^-$ takes place due to the symmetric stretch of iodine molecules [20]. So during the heating process, the lengthening of I(4B)–I(5B) distances of I_2 units to 2.77 Å transforms the disordered atoms I(4B), I(5B) with minor occupancies to that with the main occupancies I(4A), I(5A). The Raman band corresponding to interiodine distance I(1)–I(2) = 3.003 Å of the I_3^- units, according to the above v(I–I) vs. d(I–I) correlation is located at frequencies smaller than that of 100 cm^{-1} which was not possible to detect in this low-frequency region. At 160 °C the peak at 168 cm^{-1} with increased intensity corresponds to new charge transfer interactions between the I_2, I_3^- units produced by the decomposition of the sample.

The displacement of I(4B), I(5B) atoms of I_2 units as a result of a charge transfer interaction $I_2 \cdots I_3^-$ changes the distribution of electronic density which remains localized since there is no interaction between the subsequent I_7^- units (I(5)–I(5) = 4.50 Å) [3] and has very little contribution to the conductivity. The second topical maximum value of the conductivity at 399.7 K, corresponds to the sublimation of iodine molecules which shortens the I(5)–I(5) distances of the subsequent heptaiodide ions providing conductive paths for the localized charges [21]. The above description explains the experimental results at temperature dependence of ac-conductivity and Raman spectra.

Similar behaviour is observed for the β-Li inclusion compound. The conductivity starts deviating from the exponential behaviour at $T > 353$ K (80 °C) taking the maximum value $3.95 \times 10^{-7}\,\Omega^{-1}\,cm^{-1}$ at 361.8 K and the secondary maximum value $5.63 \times 10^{-8}\,\Omega^{-1}\,cm^{-1}$ at 403 K (130 °C) (Fig. 2).

In the DSC trace of β-Li (Fig. 6), the first slab endothermic peak with onset value 108 °C over the temperature region 80–119 °C (353 K–392 K) is attributed to the removal of the easily movable water molecules. The shoulder at 119 °C (392 K) corresponds to the tightly bound water molecules that are totally removed until the temperature 127 °C. At 129 °C (402 K) the sublimation of

iodine starts, which is responsible for the topical maximum value of the conductivity at 403 K (Fig. 2) and for the shoulder of the DSC trace at 129 °C (Fig. 6). In the Raman spectra of β-Li the peaks at 179 and 165 cm^{-1} are explained in the same way as was discussed for the β-K sample. Additionally, the band at 163 cm^{-1} reveals an intermediate state of the lengthening of iodine molecules during the charge transfer interactions. At 150 °C the peaks at 168 and 163 cm^{-1} are attributed to the new charge transfer interactions between I_2, I_3^- units.

The above results of β-K, β-Li are in agreement with those found for the β-CD polyiodide inclusion compounds with Ba^{2+}, Cd^{2+} [22] and Cs^+ [23] cations because of their isomorphous crystal structures.

5. Conclusions

(i) The Arrhenius exponential behaviour $\sigma = \sigma_0 \exp(-E_W/2K_BT)$ of the ac-conductivity for $T > 275$ K is caused by the contribution of metal cations K^+, Li^+. This contribution is facilitated by the water-net via the Grotthuss mechanism.

(ii) The ac-conductivity starts deviating from the exponential behaviour with lower increasing rate in both inclusion compounds at temperatures above 345 K approximately, since the water molecules start to escape initiating the rupture of the water-net and the restriction of the proton transportation via the Grotthuss mechanism.

(iii) β-K, β-Li show a semiconductor to metal transition at temperatures 371.1 and 361.8 K, respectively, caused by the removal of all the remaining water molecules.

(iv) The Raman peaks at 179, 170 and 165 cm^{-1} indicate charge transfer interactions in the I_7^- units and that their negative charge remains localized with negligible contribution to the conductivity until the sublimation of iodine starts.

(v) The sublimation of I_2 causes topical maximum values of the conductivity at 399.7 K for β-K and 403 K for β-Li.

Acknowledgement

This work was partly supported by Grant No. 70/4/3347SARG, NKUA.

References

[1] M. Noltemeyer, W. Saenger, X-ray studies of linear polyiodide chains in α-cyclodextrin channels and a model for the starch–iodine complex, Nature 259 (1976) 629–632.

[2] M. Noltemeyer, W. Saenger, Structural chemistry of linear α-cyclodextrin–polyiodide complexes. X-ray crystal structures of (α-cyclodextrin)$_2 \cdot LiI_3 \cdot I_2 \cdot 8H_2O$ and (α-cyclodextrin)$_2 \cdot Cd_{0.5} \cdot I_5 \cdot 27H_2O$, models for the blue amylose—iodine complex, J. Am. Chem. Soc. 102 (1980) 2710–2722.

[3] C. Betzel, B. Hingerty, M. Noltemeyer, G. Weber, W. Saenger, (β-cyclodextrin)$_2 \cdot KI_7 \cdot 9H_2O$. Spatial fitting of a polyiodide chain to a given matrix, J. Incl. Phenom. 1 (1983) 181–191.

[4] T.C. Ghikas, J.C. Papaioannou, Dielectric relaxation of α-cyclodextrin–polyiodide complexes (α-cyclodextrin)$_2 \cdot LiI_3 \cdot I_2 \cdot 8H_2O$ and (α-cyclodextrin)$_2 \cdot Cd_{0.5} \cdot I_5 \cdot 26H_2O$, Mol. Phys. 100 (2002) 673–679.

[5] J.C. Papaioannou, T.C. Ghikas, Dielectric relaxation of α-cyclodextrin–polyiodide complexes α-cyclodextrin)$_2 \cdot BaI_2 \cdot I_2 \cdot 8H_2O$ and (α-cyclodextrin)$_2 \cdot KI_3 \cdot I_2 \cdot 8H_2O$, Mol. Phys. 101 (2003) 2601–2608.

[6] J.C. Papaioannou, Dielectric relaxation of β-cyclodextrin–polyiodide complexes (β-cyclodextrin)$_2 \cdot LiI_7 \cdot 8H_2O$ and (β-cyclodextrin)$_2 \cdot KI_7 \cdot 8H_2O$, Mol. Phys. 102 (2004) 95–99.

[7] C. Betzel, W. Saenger, B.E. Hingerty, G.M. Brown, Circular and flip-flop hydrogen bonding in β-cyclodextrin undecahydrate: a neutron diffraction study, J. Am. Chem. Soc. 106 (1984) 7545–7557.

[8] V. Zabel, W. Saenger, S.A. Mason, Neutron diffraction study of the hydrogen bonding in β-cyclodextrin undecahydrate at 120 K: from dynamic flip-flops to static homodromic chains, J. Am. Chem. Soc. 108 (1986) 3664–3673.

[9] A.M.G. Moreira da Silva, T. Steiner, W. Saenger, J.M.A. Empis, J.J.C. Teixeira-Dias, Hydration and dehydration processes of β-cyclodextrin: a raman spectroscopic study, J. Incl. Phenom. Macro. Chem. 25 (1996) 21–24.

[10] J.C. Papaioannou, N.D. Papadimitropoulos, I.M. Mavridis, Dielectric relaxation of β-cyclodextrin complex with 4-*t*-butylbenzyl alcohol, Mol. Phys. 97 (1999) 611–627.

[11] G. Nolze, W. Kraus, PowderCell 2.0 for Windows, Powder Diffr. 13 (1998) 256–259.

[12] G. Patermarakis, J. Papaioannou, H. Karayianni, K. Masavetas, Interpretation of electrical conductance transition of hematite in the spin-flip magnetic transition temperature range, J. Electr. Soc. 151 (2004) 62–68.

[13] J. Ross Macdonald, Impedance Spectroscopy, Wiley, New York, 1987, pp. 252.

[14] B.V. Merinov, Mechanism of proton transport in compounds having a dynamically disordered hydrogen bond network, Solid State Ionics 84 (1996) 89–96.

[15] N. Agmon, The Grotthuss mechanism, Chem. Phys. Lett. 244 (1995) 456–462.

[16] P. Svensson, L. Kloo, Synthesis, structure, and bonding in polyiodide and metal iodide–iodine systems, Chem. Rev. 103 (2002) 1649–1684.

[17] L. Kloo, J. Rosdahl, P. Svensson, On the intra- and intermolecular bonding in polyiodides, Eur. J. Inorg. Chem. (2002) 1203–1209.

[18] F. Demartin, P. Deplano, F.A. Devillanova, F. Isaia, V. Lippolis, G. Verani, Conductivity, FT-Raman spectra, and X-ray crystal structures of two novel $[D_2I]I_n$ ($n = 3$ and D = *N*-Methyl-benzothiazole-2(3H)-selone; $n = 7$ and D = *N*-Methyl-benzothiazole-2(3H)-thione) iodonium salts. First example of $I^- \cdot 3I_2$ heptaiodide, Inorg. Chem. 32 (1993) 3694–3699.

[19] A. Anderson, T.S. Sun, Raman spectra of molecular crystals I. Chlorine, bromine, and iodine, Chem. Phys. Lett. 6 (1970) 611–616.

[20] P. Svensson, L. Kloo, A vibrational spectroscopic, structural and quantum chemical study of the triiodide ion, J. Chem. Soc. Dalton Trans. (2000) 2449–2455.

[21] A. Oza, Electrical-conduction in organic polyiodide chain complexes, Cryst. Res. Technol. 19 (1984) 697–707.

[22] V.G. Charalampopoulos, J.C. Papaioannou, Correlation of dielectric properties, Raman spectra and calorimetric measurements of β-cyclodextrin–polyiodide complexes (β-cyclodextrin)$_2 \cdot BaI_7 \cdot 11H_2O$ and (β-cyclodextrin)$_2 \cdot CdI_7 \cdot 15H_2O$, Mol. Phys. 103 (2005) 2621–2631.

[23] V.G. Charalampopoulos, J.C. Papaioannou, H.S. Karayianni, Dielectric and Raman spectroscopy of the heptaiodide complex (β-cyclodextrin)$_2 \cdot CsI_7 \cdot 13H_2O$, Solid State Sci. 8 (2006) 97–103.